PHOTOMETRIC AND SPECTRAL ANALYSIS OF THE OPTICAL COMPANION TO SAX J2103.5+4545

A THESIS SUBMITTED TO
THE GRADUATE SCHOOL OF NATURAL AND APPLIED SCIENCES
OF
MIDDLE EAST TECHNICAL UNIVERSITY

BY

SİNEM ÖZBİLGEN

IN PARTIAL FULFILLMENT OF THE REQUIREMENTS
FOR
THE DEGREE OF MASTER OF SCIENCE
IN
PHYSICS

DECEMBER 2008

Approval of the thesis:

PHOTOMETRIC AND SPECTRAL ANALYSIS OF THE OPTICAL COMPANION TO SAX J2103.5+4545

submitted by **SİNEM ÖZBİLGEN** in partial fulfillment of the requirements for the degree of **Master of Science in Physics Department, Middle East Technical University** by,

Prof. Dr. Canan Özgen
Dean, Graduate School of **Natural and Applied Sciences** _____

Prof. Dr. Sinan Bilikmen
Head of Department, **Physics** _____

Prof. Dr. Ümit Kızıloğlu
Supervisor, **Physics Department, METU** _____

Examining Committee Members:

Prof. Dr. Nilgün Kızıloğlu
Physics, METU _____

Prof. Dr. Ümit Kızıloğlu
Physics, METU _____

Prof. Dr. Rikkat Civelek
Physics, METU _____

Assist. Prof. Dr. Sinan Kaan Yerli
Physics, METU _____

Assist. Prof. Dr. Sıtkı Çağdaş İnam
Electrical and Electronics Engineering, Başkent University _____

Date: _____

I hereby declare that all information in this document has been obtained and presented in accordance with academic rules and ethical conduct. I also declare that, as required by these rules and conduct, I have fully cited and referenced all material and results that are not original to this work.

Name, Last Name: SİNEM ÖZBİLGEN

Signature :

ABSTRACT

PHOTOMETRIC AND SPECTRAL ANALYSIS OF THE OPTICAL COMPANION TO SAX J2103.5+4545

Özbilgen, Sinem
M.S., Department of Physics
Supervisor: Prof. Dr. Ümit Kızıloğlu

December 2008, 34 pages

In this study spectral and photometric data of the SAX J2103.5+4545 Be/X-ray system are given. The spectral data were taken from June 2007 to September 2008 with the 1.5 m Russian-Turkish telescope, whereas the photometric data were obtained using ROTSE-IIId archive from June 2004 to November 2008. The photometric data up to April 2007 shows that the system was in quiescence in the optical region. But, in the 23^{rd} of April 2007, the system's luminosity underwent a large increase, which is in agreement with X-ray data. This increase was approximately 1 mag. Also, the Hα line was displaying an emission with increased equivalent width proportional to the outburst. Afterwards, the Hα line profile changed from a double peaked emission into a single peaked absorption, which is in agreement with the system's structure. This means that the Be star threw away its disc and its light curve fell back to its old luminosity.

Keywords: Be/X-ray Binaries, Be Stars, SAX J2103.5+4545

ÖZ

SAX J2103.5+4545 X-IŞIN PULSARININ FOTOMETRİK VE SPEKTRAL ANALİZİ

Özbilgen, Sinem
Yüksek Lisans, Fizik Bölümü
Tez Yöneticisi: Prof. Dr. Ümit Kızıloğlu

Aralık 2008, 34 sayfa

Bu çalışma SAX J2103.5+4545 Be/X-ışın sisteminin optik bileşeninin Haziran 2007-Eylül 2008 arasında 1.5 metrelik Rus-Türk teleskobu ile yapılmış tayfsal gözlemleri ve Haziran 2004-Kasım 2008 arasında ROTSE-IIId arşivi kullanılarak elde edilmiş fotometrik gözlemleri yer almaktadır. Nisan 2007'ye kadar olan fotometrik veriler sistemin optik bölgede durgun bir dönemde olduğunu göstermektedir. Ancak 23 Nisan 2007'de kaynağın parlaklığında X-ışın bölgesindeki verilerle uyumlu hızlı bir artış olduğu gözlemlenmiştir (Galis, R., et al. ATel#1063). Bu artış miktarının 1 kadire kadar yükseldiği saptanmıştır. Bunun yanısıra tayflarda bulunan Hα çizgilerinin emisyon durumunda olduğu ve eşdeğer genişliğinin patlama ile orantılı arttığı görülmüştür. Devamında ise Hα çizgi profili çift tepeli emisyondan tek tepeli absorbsiyon çizgisine dönmüştür ki bu sistemin yapısıyla tutarlıdır. Yani Be yıldızı patlamayla birlikte etrafındaki diskini atmiş ve ışık eğrisi tekrar eski parlaklığına düşmüştür.

Anahtar Kelimeler: Be/X-Işın Çiftleri, Be Yıldızları, SAX J2103.5+4545

To my dearie husband

ACKNOWLEDGMENTS

First of all I'd like to thank my advisor Prof. Dr. Ümit Kızıloğlu for letting me have the opportunity to work with him. Also, I am very grateful to Prof. Dr. Nilgün Kızıloğlu, Assist. Prof. Dr. Sinan Kaan Yerli and Assist. Prof. Dr. Sıtkı Çağdaş İnam for their comments and all their help.

I give my heartfelt thanks to my friends Pınar Yılmaz, Nadir Ghazanfari, İlker Doğan, Mehmet Umut Çağlar, Tuğba Bolat, Elif Beklen, Özlem İpek, Nora Nayir, Tuğba Yılmazer and members of METU Amateur Astronomy Society and METU Physics Society for not leaving me alone and providing help and friendship during the master years. Also, I would like to thank Mehtap Özbey for sharing information about the methods used in the thesis and for always supporting me. I also thank K. Başar Coşkunoğlu for helping me write the thesis and overcome the difficulties I've faced when writing it.

My final thanks go to my Bayar and Özbilgen families for never stopping supporting and/or encouraging me in this remotely executed study. I am gratefull to my dear sister Gizem Bayar for her interest and endless help and support. Also, I am grateful to my other family, who permitted me to stay with them each time I traveled to Ankara: Akif Ersoy, Cansel Ersoy, Engin Günaltay and especially Jale Ersoy, who supported me from the very start, who got tired with me when it was hard for me, who cried with me when I was feeling sorry and who endured all my whims. Finally, I give my thanks and love to my dear husband Cenk Özbilgen for always helping me, for making me work comfortably and for always loving me.

I also acknowledge The Scientific and Technological Research Council of Turkey (TUBITAK) for their funds.

TABLE OF CONTENTS

LIST OF TABLES

TABLES

LIST OF FIGURES

FIGURES

CHAPTER 1

INTRODUCTION

In Chapter 1, a brief history of Be/X-ray binaries and a literature scan is given. Also in Chapter 1, information regarding the formation of Be/x-ray binaries and the most popular disc model (Viscous Decretion Disc Model) are explained. In Chapter 2, background, photometric and spectroscopic data about SAX J2103.5+4545 were discussed. The reduction methods of photometric and spectroscopic data are also in this chapter. Finally, the results obtained analyzing the data are presented as well. In Chapter 3, the findings of the study are summarized.

1.1 Be/X-ray Binaries

Be/X-ray binaries comprise the largest of High Mass X-ray Binaries (HMXBs). About %70 of known HMXB systems fall into this category. Be/X-ray binaries consist of a Be star and a neutron star (Figure 1.1). The Be star is used as a general term, describing an early type (as late as B2) non supergiant star, which, at some time, shows emission in the Balmer series lines (Collins 1987, Slettebak 1988). Another property of these stars is that they show strong infrared excess. These two properties are attributed to the presence of a circumstellar disc. The orbits of Be/X-ray binaries are highly wide and eccentric (e ~ 0.1-0.9) with relatively long periods (P_{orb} ~ 17-263 d) (Ziółlkowski 2002). The optical component is not substantially evolved and its Roche lobe is not full.

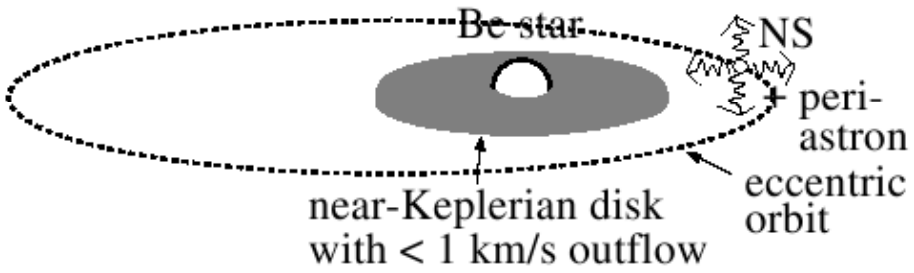

Figure 1.1: Picture describing a Be/x-ray binary (Okazaki and Negueruela 2001)

1.1.1 X-ray Behaviour in Be/X-ray Binaries

Be/X-ray binaries present two different kinds of X-ray behaviour (Stella et al. 1986, Neguerula 2004, Reig and Roche 1999, Okazaki and Negueruela 2001):

- Persistent X-ray sources displaying low X-ray luminosity at a relatively constant level ($L_x \sim 10^{34}$ ergs^{-1}). The intensity of the luminosity can vary by up to 10 times (Figure 1.2a).

- Most known Be/X-ray binaries undergo outbursts in which the X-ray luminosity suddenly increases by more than 10 times. These systems are called Be/X-ray transients. Be/X-ray transients undergo two types of outbursts:

  a) X-ray outbursts of moderate intensity ($L_x \sim 10^{36}$ - 10^{37} ergs^{-1}), which are also known as Type I outbursts. These generally occur when the neutron star passes through the periastron (Figure 1.2b), and last from several days to a week. The outbursts reoccur on multiples of orbital periods, but not necessarily every time the neutron star passes through the periastron. Sometimes the flares do not happen at all or they are unusually weak when they do. In some systems the outbursts can disappear for years or decades. Most Be/X-ray binaries show Type I outbursts occasionally, but their patterns differ from each other. Some systems produce these during almost every periastron passage, whereas some other systems produce

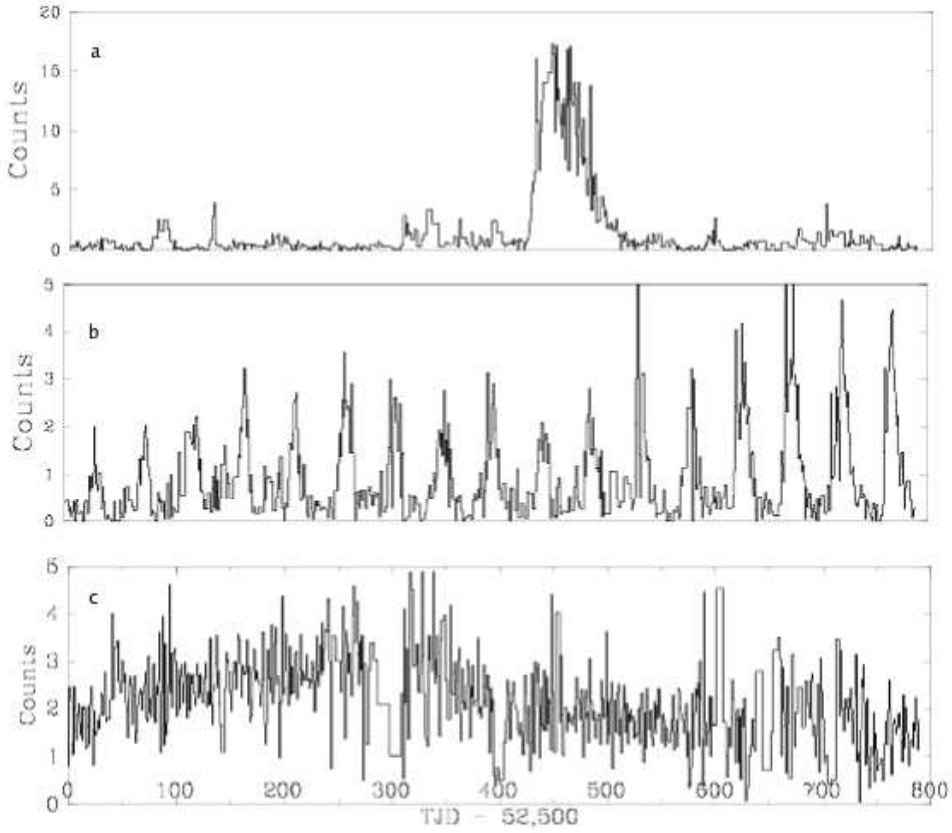

Figure 1.2: All light curves were taken with ASM on board of Rossi XTM (a) Light curve of persistent X-ray source X Persei. The sharp peaks are due to either low signal-to-noise points or solar contamination. X Persei is also the closest Be/X-ray binary ($L_x \sim 10^{34}$ - 10^{35} ergs^{-1}). (b) Light curve of EXO 2030+375 showing a long series of Type I outburst close to the time of periastron passage ($L_x \sim 10^{37}$ ergs^{-1}). (c) The Be/X-ray transient X0656-072 displays a Type II outburst after approximately 30 years in quiescence ($L_x \sim 10^{38}$ ergs^{-1}) (Negueruela 2004).

it very rarely. In the latter group Type I outbursts are seperated by long periods; in which only Type II outbursts take place.

b) Giant X-ray outbursts of severe intensity ($L_x \gtrsim 10^{37}$ ergs^{-1}) also known as Type II outbursts which last for several weeks or even months. Most of the time Type II outbursts start shortly after the periastron passage of the neutron star, but do not show any other correlation with orbital parameters (Finger and Prince 1997) (Figure 1.2c). They occur irregurlarly but the typical recurrence time is of the order of several years. Before a Type II outburst takes place, emission lines are usually enhanced, which means

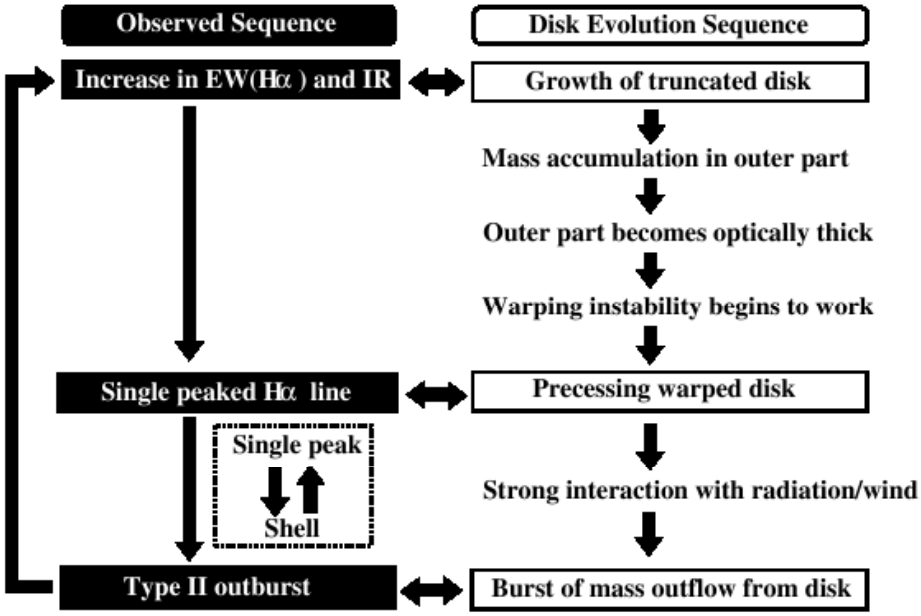

Figure 1.3: The observed cyclic activity of a Be/X-ray binary system and the corresponding Be disc evolution sequence explaining the mechanism of a Type II outburst (Okazaki and Negueruela, 2001).

the activity of the Be star has increased.

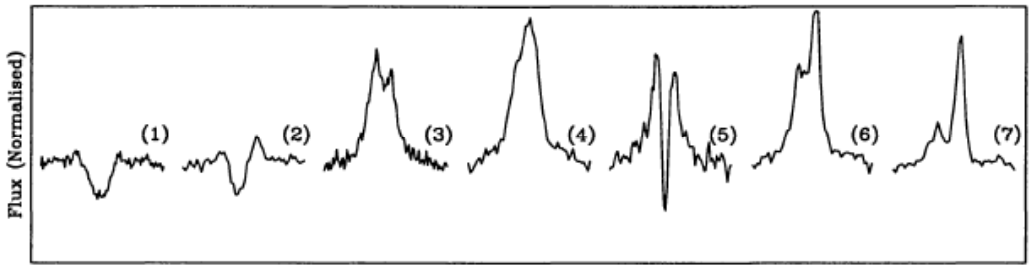

Figure 1.4: H-alpha line profile from 1995 to 1998 for V 635 Cas. In (1), there is no decretion disc around the Be star, because the line profile just shows an absorption originated from the star. In (2), the presence of the disc can be detected, because there is a small emission in the line profile. (3) shows a double-peak. In (4), the peaks converge until there is only one peak in the profile, which indicates that the disc is warping. The sharp absorption in the middle of the line indicates that the warped disc is precessing (5). Finally, in (6 and 7) the disc becomes very perturbed and the strength of the emission line decreases, which leads to a new disc-less phase (Negueruela and Okazaki, 2000).

According to Okazaki and Neguerula (2001), a Be/X-ray binary system loses its decretion disc after a few Type II outbursts. They proposed the following scenario as a possible Type II outburst mechanism (Figure 1.3): After the disc is lost the material ejected from the Be star starts to accumulate around it, forming a new disc. As more matter accumulates on the disc, its emission increases. Even though the star keeps supplying the disc with matter, the outflow of gas is blocked at a certain radius. This leads to the accumulation of gas in the outermost part of the disc, and in time, the optically thin disc becomes thick. Since an optically thick disc is weak to radiation-driven warping it starts to warp and precess (Pringle 1996, Porter 1998). As the warped disc precesses, the shape of the line profile changes (Figure 1.4). The disc's warped region will interact with the stellar wind and radiation. The interaction will deform and elongate the disc's outer part. This will make the disc lose a large amount of matter, which will fall onto the neutron star causing a Type II outburst. After loosing a big portion of its mass, the disc will become fainter. It is trivial to deduce that the decretion disc around the Be star plays the most important role in X-ray behaviour of Be/X-ray binaries.

1.1.2 Corbet Diagram

Corbet (1984, 1986) found that the observed X-ray pulse periods for Be/X-ray binary systems are strongly correlated to their periods (Figure 1.5). This correlation is an expected one, because the neutron star tries to adjust its spin period to the equilibrium value. This equilibrium period is defined as the spin period for which the corotation velocity at the magnetospheric radius equals the Keplerian velocity. The equilibrium periods value increases as the flux of the matter supply to the vicinity of the neutron star decreases ($P_{equ} \sim \dot{M}^{-3/7}$). In wide systems with long orbital periods the accretion is fed from the outer parts of the decretion disc and expected mass flux is low. Obviously, this leads to long spin periods.

When the spin period is greater than the equilibrium period the neutron star reaches the equilibrium period via angular momentum transfer from the accretion disc around the neutron star. In the case of the spin period being less than the equilibrium period the matter which tries to accrete on the neutron star is driven away by the stellar wind

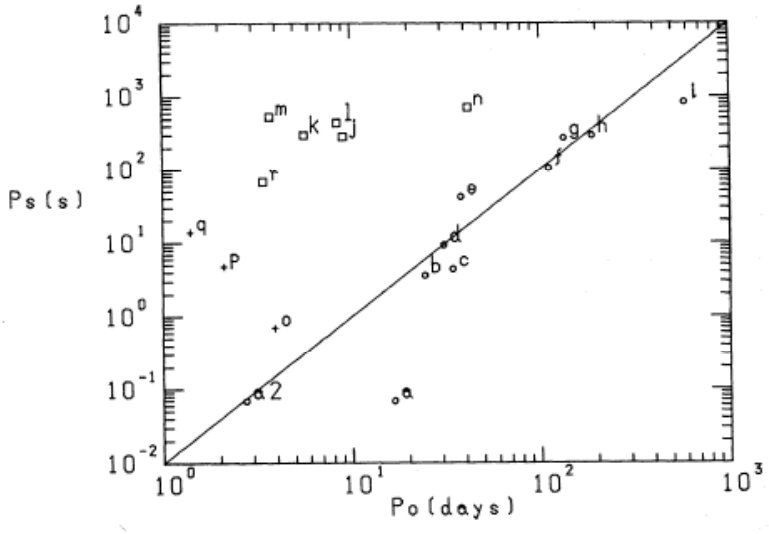

Figure 1.5: Orbital period versus spin periods for binary systems, with a neutron star component (HMXB), showing X-ray activity. Systems from a to e (circles) have Be type primaries, from j to n (squares) the primaries are supergiants and finally o,p and q (plus symbol) probably have Roche lobe filling binaries. The straight line indicates an empirical approximation to the relationship between orbital and spin periods for Be/X-ray binaries, except for a, assuming e = 0.7 (Corbet 1986).

with low angular momentum. Therefore, an accretion disc around the neutron star cannot be formed. The driving away of the matter leads to angular momentum transfer from the neutron star to the matter. Thus making the neutron star's spin slower and increasing its spin period (Li and van den Heuvel 1996, Waters and Kerkwijk 1989, Apparao 1994).

Ziolkowski (2002) improved Corbet's diagram. His version of the diagram contains 25 Be/X-ray binaries and correlation can be seen more clearly (Figure 1.6).

1.2 Formation of Be/X-Ray Binaries and Viscous Disc Model

1.2.1 Formation of Be/X-Ray Binaries

Be/X-ray binaries evolve from a close pair of early B type stars. The more massive star will, of course, evolves first and fills its Roche lobe, then starts transferring mass to its companion. The companion's mass and angular momentum increase which

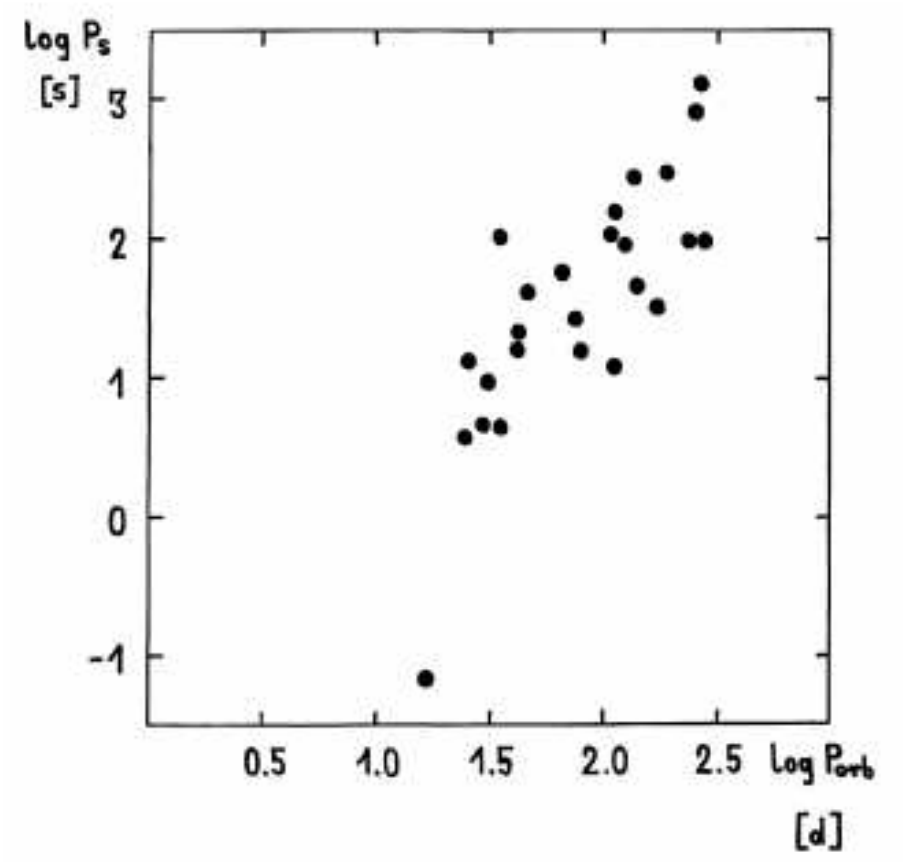

Figure 1.6: Ziolkowski's improved Corbet diagram. This diagram contains 25 systems whereas Corbet's original diagram contains 9 Be/X-ray binaries (Ziolkowski 2002).

leads to a fast rotating B star, which can become a Be star. The mass losing B star evolves even further and leaves a compact object behind, forming a Be star-compact object binary. Since the evolving star is a B type star ($M_{initial}$ > 4-8 $M_{\odot}$) it can only become a neutron star due to mass restriction (Figure 1.7.) (Rappaport and van den Heuvel 1982, de Loore et al. 1982, Apparao 1994).

1.2.2 Viscous Decretion Disc Model

A Be star has two-component extended atmosphere, a polar region and a relatively cool (~104 °K) equatorial disc. There are several models, which try to understand the nature of this disc. Among them the only one, which can explains the near-Keplerian

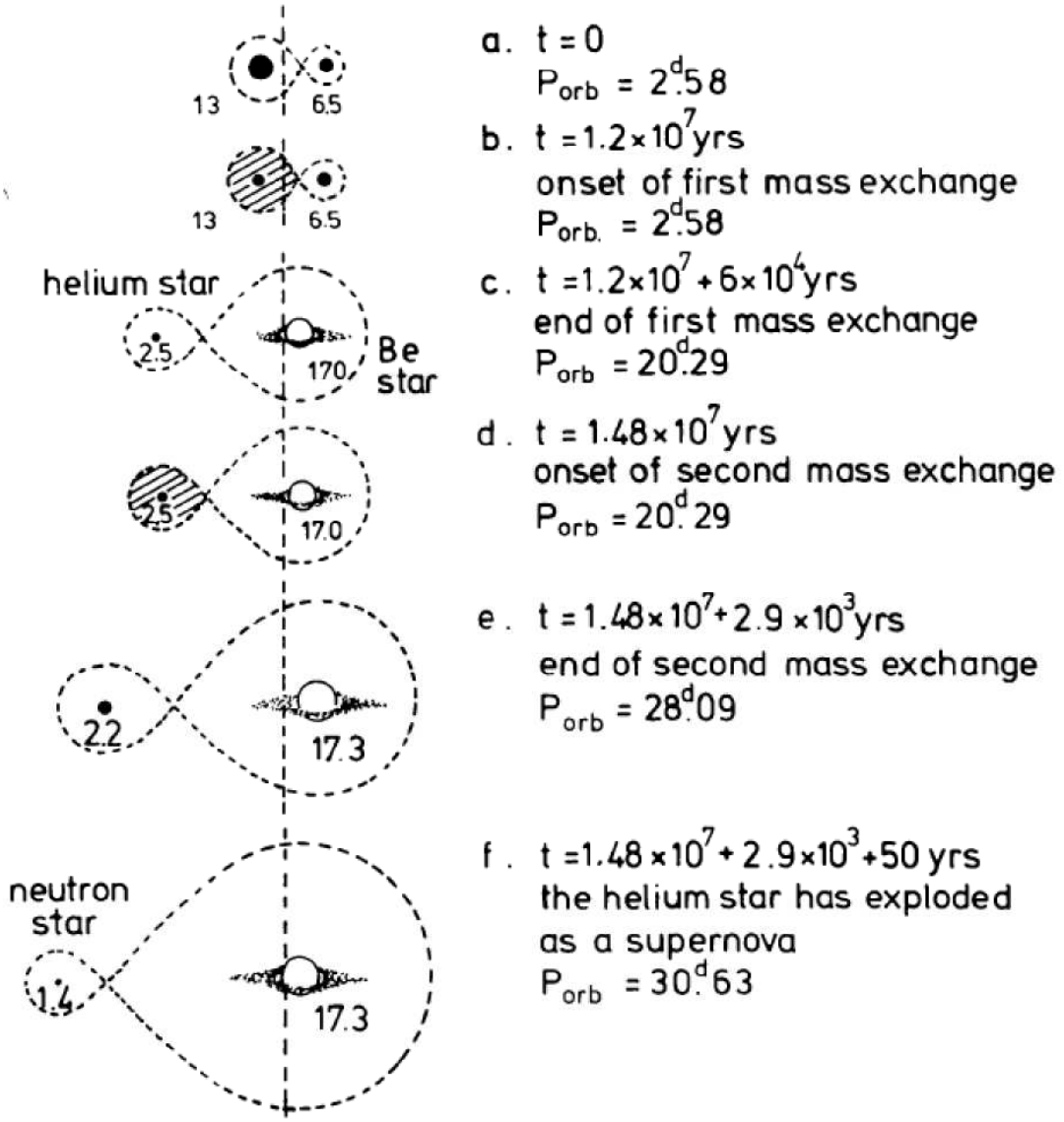

Figure 1.7: Formation of Be star - compact object binary from evolution of a binary system with initial masses of the stars M_1 = 13 $M_\odot$ and M_2 = 6.5 $M_\odot$ (Habets, 1986).

discs, is the viscous decretion disc model (here after VDDM) proposed by Lee et al. (1991). In VDDM, matter supplied from the equatorial surface of the star gradually drifts outward by the viscous torque and forms the disc (Figure 1.8) (Okazaki 2001, 2006). According to VDDM, the star transfers angular momentum to the inner region of the disc, increasing its angular velocity to Keplerian. The mechanism for this transfer is still unknown. Then, viscosity conducts material outwards. This behaviour of the disc is the opposite of an accretion disc and therefore it is called a decretion disc.

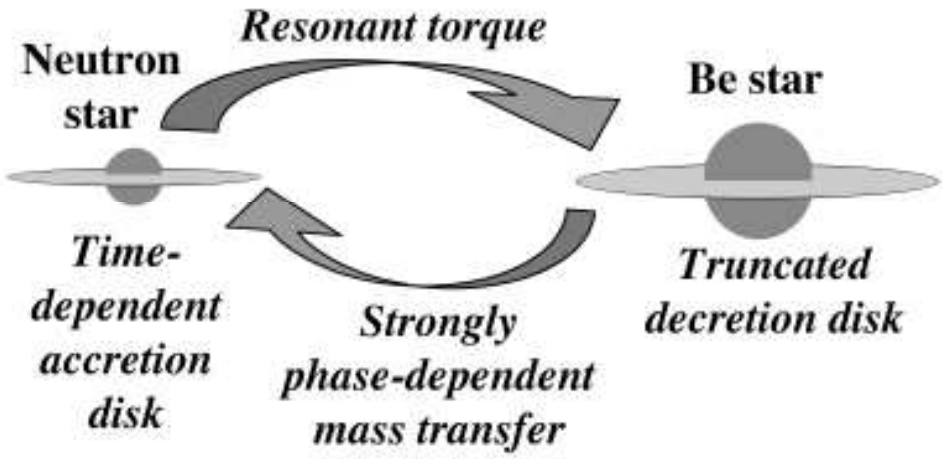

Figure 1.8: Schematic diagram of the interactions in Be/X-ray binaries (Okazaki and Hayasaki 2006).

The outflow speed is inversely proportional to the viscosity of disc matter, namely, the more viscous the disc matter is, the slower its outflow speed will be.

CHAPTER 2

SAX J2103.5+4545

2.1 History of SAX J2103.5+4545

SAX J2103.5+4545 was discovered in 1997 by Hulleman et al. with Wild Field Camera (WFC) on board of BeppoSAX X-ray satellite. The system was active from February to September 1997. The peak intensity of 20 mCrab (2 to 25 keV) was observed on the 11th of April. The pulse period around the time of the peak was 358.61± 0.03 s on MJD 50569. It's equatorial coordinates in J2000 is $\alpha = 21^h\ 03^m\ 33^s$ and $\delta = 45^\circ\ 45'.0$ (Hulleman, in't Zand and Heise, 1998).

The second study regarding the system (Baykal, Stark and Swank, 2000) made use of ASM data (like most other studies). ASM detected another outburst on the 25th of October 1999, which reached a peak X-ray brightness of 27 mCrab on the 28th of October 1999 (Figure 2.1). They calculated the eccentricity as e=0.4 ± 0.2 with an orbital period of 12.68 ± 0.25 days. The pulse period they measured was in agreement with Hulleman, in't Zand and Heise (1998). The same group measured the distance of the system as ~3.2 kpc and its surface magnetic field as 1.2 x 1013 G.

Lutovinov, Molkov and Revnivtsev (2003) were the first group to study the system with INTEGRAL data. They measured the energy the system emits as up to 100 keV. The values they found were in agreement with previous studies.

Reig et al. (2004) identified the pulsar's optical counterpart (Figure 2.2). They discovered that the optical companion is a B0e spectral type main sequence star. Its V band magnitude is measured as V=14.2. The amount of reddening was estimated as

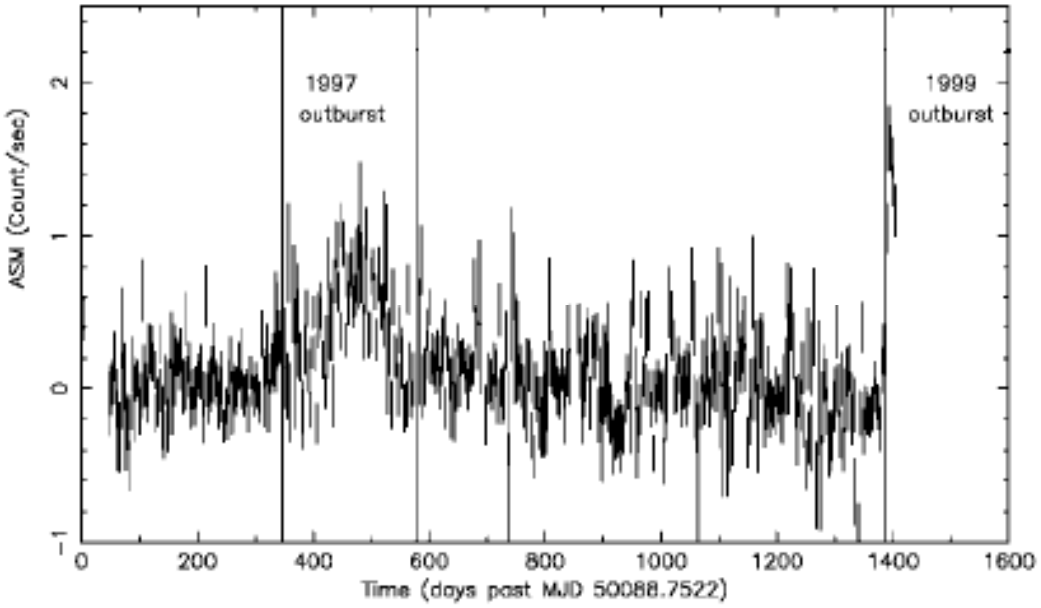

Figure 2.1: Light curve of ASM data (Baykal, Stark and Swank, 2000)

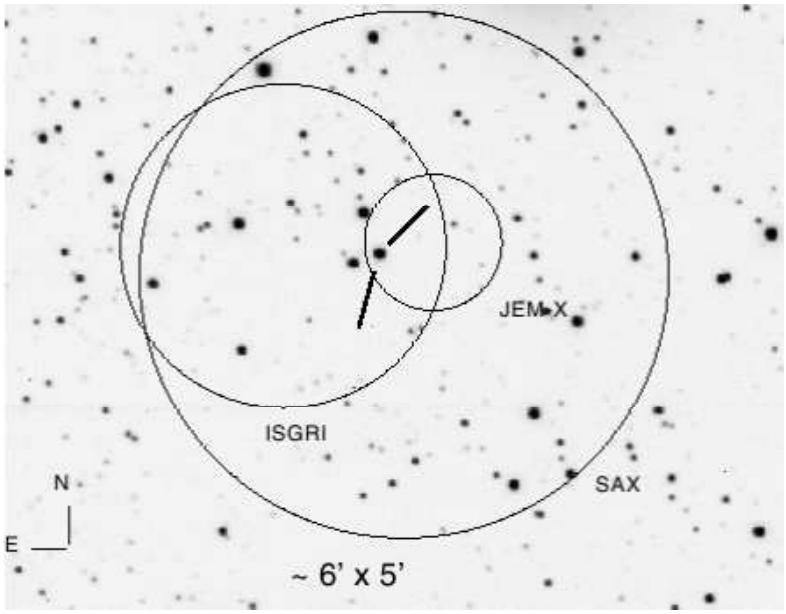

Figure 2.2: Optical V filter image of the field around SAX J2103.5+4545, with X-ray position uncertainty circles from the WFC onboard BeppoSAX and ISGRI and JEM-X onboard INTEGRAL. The coordinates of the proposed optical counterpart are $\alpha = 21^h\ 03^m\ 35.7^s\ \delta = 45^\circ\ 45'.0\ 04''$ (Eq. 2000) (Reig et al. 2004).

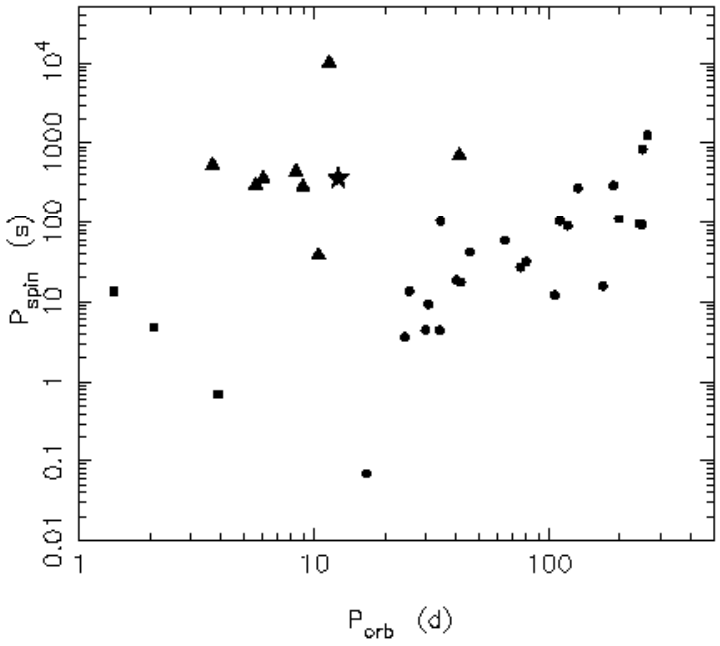

Figure 2.3: Updated Corbet's $P_{spin}-P_{orb}$ diagram. The asterisk denotes the location of the SAX J2103.5+4545. Circles represent the Be/X-ray binaries, triangles identified wind-fed supergiants and squares refer to disc-fed systems (Reig et al. 2004).

$A_V = 4.2 \pm 0.3$ magnitude, which implies a distance of d $\simeq 6.5 \pm 0.9$ kpc. The orbital period they determined is in agreement with previous studies and this result identifies the system as the Be/X-ray binary with the shortest orbital period by the of the study was made. Figure 2.3 representes an updated Corbet's diagram. In this figure, the star symbol denotes SAX J2103.5+4545 which is seen among the wind-fed supergiants. And they also showed Hα line profile obtained from their observations in 2003. The spectra had a variable Hα emission line (Figure 2.4).

In 2004, Blay et al. measured the X-ray luminosity of the system as 3.5 x 10^{36} ergs^{-1}

Table 2.1: Orbital parameters of SAX J2103.5+4545 (Baykal et al. 2007).

Parameter	Value
$T_{\pi/2}$Orbital Epoch (MJD)	52469.336±0.057
P_{orb} (days)	12.66536±0.00088
Eccentricity e	0.4055±0.0032
Longitude of periastron w (deg)	244.3±6.0

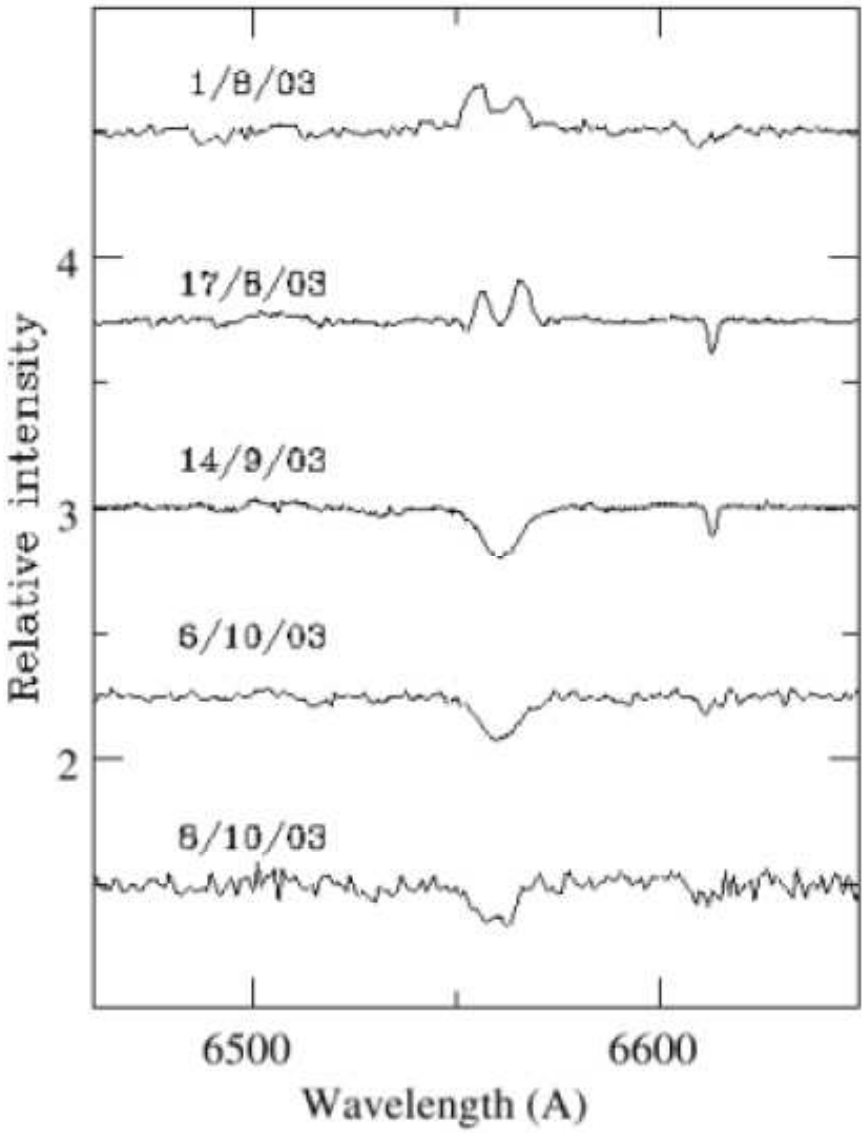

Figure 2.4: Evolution of Hα line in 2003 (Reig et al. 2004).

in the 10-100 keV energy range, which means the system underwent a Type I outburst. Flippova et al. (2004) reevaluated the equatorial coordinates of the system $\alpha = 21^h$ 03^m 36^s $\delta = 45^\circ$ $45'.0$ $45''$. Baykal et al. (2007) obtained revised orbital parameters (Table 2.1). Reig (2004), Blay et al. (2004), Inam et al. (2004), Sidoli et al. (2004, 2005), Blay et al (2006), Camero Arranz (2007) also published studies about the system in X-rays which generally agree on parameters given earlier.

Figure 2.5: Robotic Optical Transient Search Experiment (ROTSE)

2.2 Observational Instruments

2.2.1 Photometric Observations Instrument

Optical component of SAX J2103.5+4545 was photometrically observed with Robotic Optical Transient Search Experiment[1] (ROTSE) in Turkish National Observatory (TUG) in Antalya, Turkey. The ROTSE project is trying to observe Gamma-ray (GRB) and X-ray bursts in the optical region. To carry out this plan several fully-automated telescopes were installed to various locations in the world. The one in Turkey is the fourth ROTSE-III telescope (Figure 2.5).

The telescope is a modified Cassegrain, which has a primary mirror with radius r=45 cm and focal ratio f/1.80. The back-illuminated, 2048x2048 pixel CCD has a 1.85x1.85 degree field of view (fov); its pixel scale is 3.28 arcsecpixel^{-1}. The system operates without filters and has a wide pass band which peaks at 550nm (Akerlof et al., 2003).

[1] http://www.rotse.net, last visited on December 2008

Figure 2.6: Russian-Turkish Telescope (RTT150)

2.2.2 Spectroscopic Observations Instrument

The 1.5 m Russian-Turkish Telescope[2] (RTT150) was used for SAX J2103.5+4545's optical component's spectroscopic observations. The telescope is a joint project of TUG, Kazan State University and Moscow Space Research Institude of Russian Academy of Sciences (Figure 2.6). It has a Ritchie-Chretien optic system. It can be used with both Cassegrain and Coude focus systems.

TFOSC (Turkish Faint Object Spectrometre and Camera) is used at f/1.7 focus on RTT150. It can be used both for direct imaging and as a low dispersion spectrometre (Figure 2.7). It has a 2048x2048, 15 μ pixel CCD. The CCD's fov is 13x13 arcmin, its pixel scale is 0.39 arcsecpixel^{-1}. There are several grisms available for use for TFOSC: *G7, G8, G9, G10, G11, G12, G14, G15, G17. G8* and *G14* were used in this

[2] http://www.tug.tubitak.gov.tr, last visited on December 2008

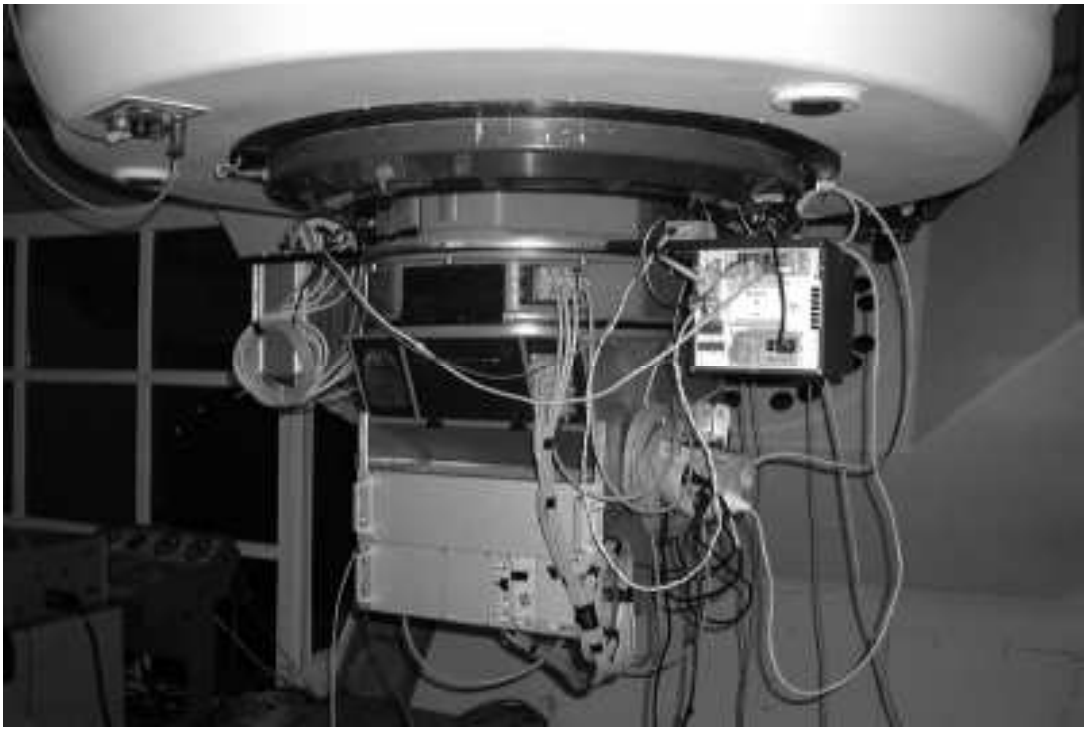

Figure 2.7: Turkish Faint Object Spectrometre and Camera (TFOSC)

study. Their properties are as follows in Table 2.2.

The 67 μ slit was also used in spectroscopic observations. This translates into an angular separation of 1.74 arcsec. Also, several spectral lamps were used for calibrations. The halogen lamp was used for normalization, whereas the Helium, Neon, Iron-Argon lamps were used for wavelength calibration.

Table 2.2: Properties of G8 and G14.

Grism	Wavelength Range (A°)	Resolution	Spectral Region
G8	6200 – 7850	2189	Red
G14	3270 – 6120	1337	Blue

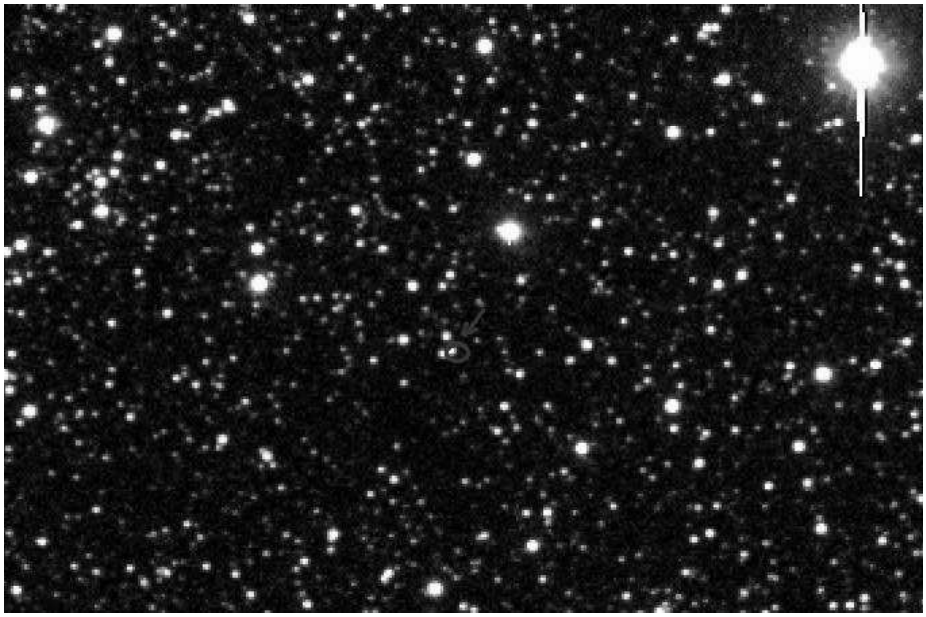

Figure 2.8: Image of SAX J2103.5+4545 taken with ROTSE on 1 April 2007.

2.3 Optical Observations

2.3.1 Optical Photometric Observations

ROTSE-IIId has been gathering photometric data of the SAX J2103.5+4545 since June 2004 (MJD 53167). The telescope did not observe the system from August 2005 to April 2007, because there were any expected outbursts. Then, it started observing the system again and still keeps doing so. Approximately 5000 data sets were collected from June 2004 to December 2007 (MJD 53167-54437) with 5 second exposure time. After the images are obtained ROTSE automatically takes dark and flat pictures and reduces the frames accordingly. The data sets up to December 2007 were analyzed thoroughly, therefore, a very precise light curve for the Be companion of the system was obtained. The newer sets were analyzed using Sextractor's aperture photometry (Bertin and Arnouts,1996), which, of course, reduced the preciseness of the light curve. As a first step instrumental magnitudes were obtained using Sextractor on the observed CCD frames. The second step was to determine ROTSE magnitudes, which were calculated by comparing the field stars with USNO A2.0 R-band

catalogue. Finally, barycentric corrections were applied to each observation's time (Kızıloğlu, Kızıloğlu and Baykal 2005).

To be able to compare the optical results with X-ray data, the All-Sky Monitor (ASM), on board of Rossi X-ray Timing Explorer (RXTE) satellite, data was obtained[3]. ASM cameras cover %70 of the sky every 1.5 hours. The data is available online in three energy bands (1.3-3.0, 3.0-5.0, 5.0-12.0 keV). In this study the 5.0-12.0 keV band's data was used (Le Vine et al., 1996).

2.3.2 Optical Spectroscopic Observations

Ten spectroscopic observations have been made with TFOSC on board of RTT150, starting from June 2007 to September 2008 (Table 2.3).

Table 2.3: Journal of optical spectroscopic observations of SAX J2103.5+4545.

Date	MJD	Grism	Exposure (s)
2007/06/14	54266.40	G8	1800
	54266.43	G14	3600
2007/07/18	54300.36	G8	1800
	54300.38	G14	1800
2007/09/13	54357.37	G8	1800
2007/10/05	54379.28	G8	1800
2007/12/14	54448.50	G8	1800
2008/06/19	54637.45	G8	1800
2008/08/26	54705.45	G8	1800
2008/09/21	54731.51	G8	1800

[3] http://xte.mit.edu, last visited on December 2008

2.4 Data Reduction and Analysis

2.4.1 Photometric Data Reduction And Analysis

Data sets were reduced using MIDAS[4] and its DAOPHOT package (Stetson 1987, 1992). First of all the fits images were minimized to 1024x1024 size (one quarter of original size). This resizing was made in order to make 'ALLSTAR' command work properly (explain in the text). For optimal use of DAOPHOT 'fits' files were converted into 'bdf'. In DAOPHOT first we execute the 'find' command to find the stars in the frame. The second step was to apply the 'photometry' command to invoke aperture photometry. Then, to determine the number of stars used in PSF the 'pick' command was ran. After that, the 'psf' function was applied to the pick stars to obtain the spread function. Finally, to determine the magnitudes of all stars except very close star couples, where the fainter one was removed from the list, the 'ALLSTAR' command was executed. The images were checked with DS9 and some were removed due to low image quality. For the rest, the coordinates of the system's optical component and the according MJD were determined and saved. The magnitudes for the nearest location to those coordinates were taken along with the relative errors. Lastly the barycentric correction was applied to MJDs.

The values entered to DAOPHOT (the units regarding the parameters were given in the bracket):

FWHM (pixel)	: 2.7
PSF Radius (pixel)	: 6.00
Gain (e^-/ADU)	: 3.00
High Good Datum (ADU)	: 32000
Threshold (σ)	: 2.00
Fitting Radius (pixel)	: 2.00
Inner Sky (pixel)	: 6.00
Outer Sky (pixel)	: 9.00

[4] http://www.eso.org/projects/esomidas, last visited on December 2008

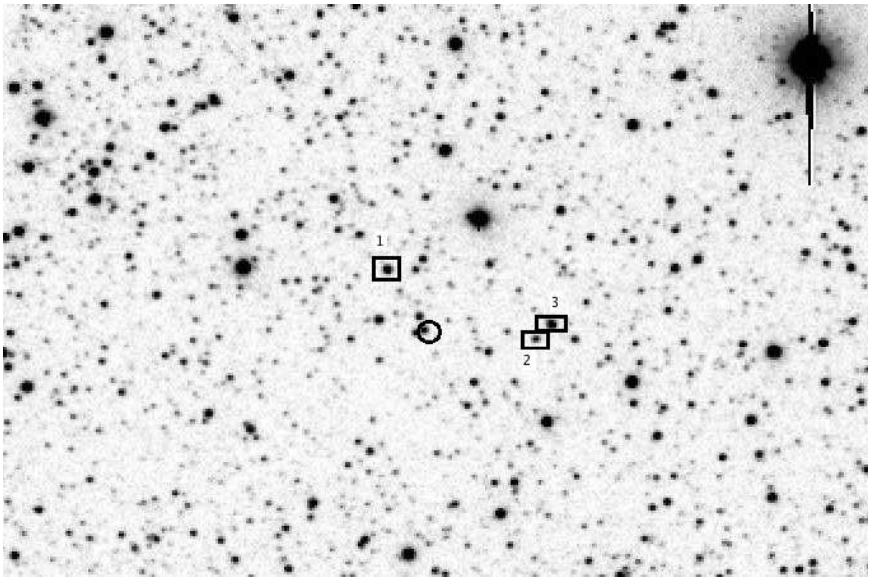

Figure 2.9: Location of the Be star and reference stars in a ROTSE image.

Three reference stars were determined by examining the system's neighbourhood, from stars with relatively constant magnitudes (Table 2.4). In Figure 2.9, SAX J2103.5 +4545 and reference stars had shown with circle and rectangular shapes. The angular seperations to the first, second and third reference stars are 1.52, 2.4 and 2.76 arcmin, respectively. The magnitudes and magnitude errors for these stars were obtained from the appropriate frames. Then the arithmetic mean magnitude was calculated for these stars. Finally, the Be star's magnitude is subtracted from the average of the reference star's to obtain the differential magnitude.

Table 2.4: Coordinates and magnitudes of the Be star and refence stars.

	α	δ	R_1 mag	R_2 mag
SAX J2103.5+4545	$21^h03^m35.7^s$	$45°45'04''$	14.63	13.65
Reference 1	$21^h03^m40.32^s$	$45°46'22.6''$	12.58	13.03
Reference 2	$21^h03^m21.99^s$	$45°44'55.5''$	13.81	14.23
Reference 3	$21^h03^m20.15^s$	$45°45'14.6''$	12.10	-

2.4.2 Spectroscopic Data Reduction and Analysis

The spectra were reduced using MIDAS and its packages; long slit and ALICE. Then, the appropriate bias, Halogen and Fe-Ar lamps images were determined by calculating the arithmetic mean of the ones with low dispersion. After that, we picked several small areas without cosmic rays and their averages were calculated. The next step was to remove the areas with higher cosmics then the median. Then, the standard bias and flat reductions were applied. The spectrum's area was extracted from the entire spectrum frame. Similarly a horizontal line, with the same width as spectrum, was also extracted from the frame. This line was used to remove to unwanted, vertical contribution to the spectrum. To obtain the x-axis values as wavelength, Fe-Ar, He and Ne lamps were used. The lamp with the best spectrum was chosen and a similar horizontal line was extracted. Then, its spectral lines were identified and calibrated accordingly, via 'APPLY/DISPERSION' command, to convert the pixels on the x-axis into wavelength. The next step was to normalize the spectrum executing 'NORMALIZE/SPECTRUM'. Lastly, to remove the effects of noise the 'FILTER/SMOOTH' command was applied. Afterwards, to determine line information the ALICE package was ran. Using ALICE, the equivalent width, full-width at half maximum and center of Hα were obtained.

CHAPTER 3

RESULTS AND DISCUSSION

Using data analysis methods mentioned before, the ~5000 data sets of SAX J2103.5 +4545 taken with ROTSE were reduced to 2372. The ROTSE magnitudes of the system's optical component were obtained using DAOPHOT (See Chapter 2.4.1). The system's light curve in Figure 3.1 shows those magnitudes plotted versus time.

In Figure 3.2, the light curves for each refence star is given along with their relative

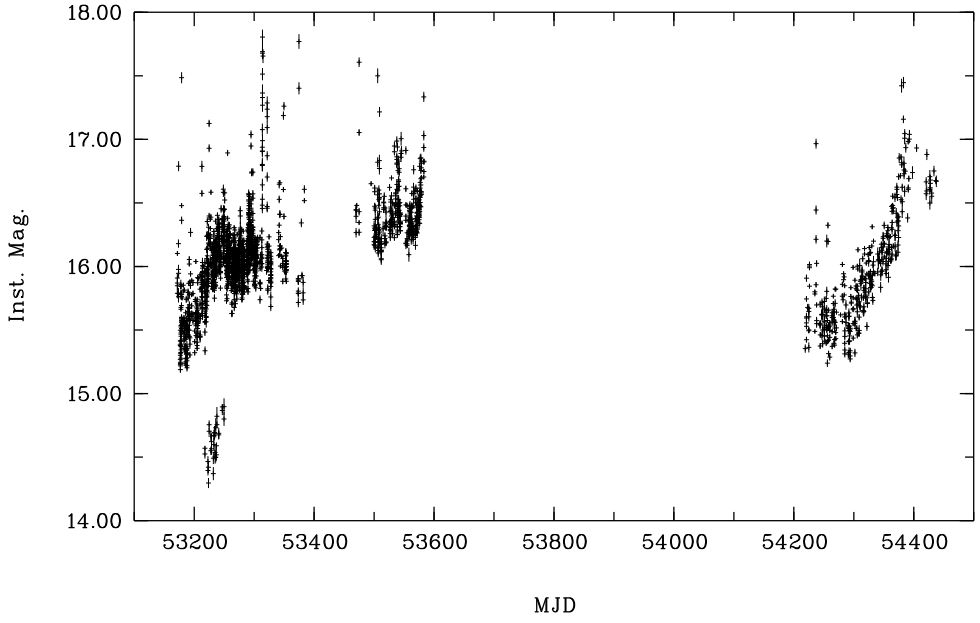

Figure 3.1: Row light curve of SAX J2103.5+4545.

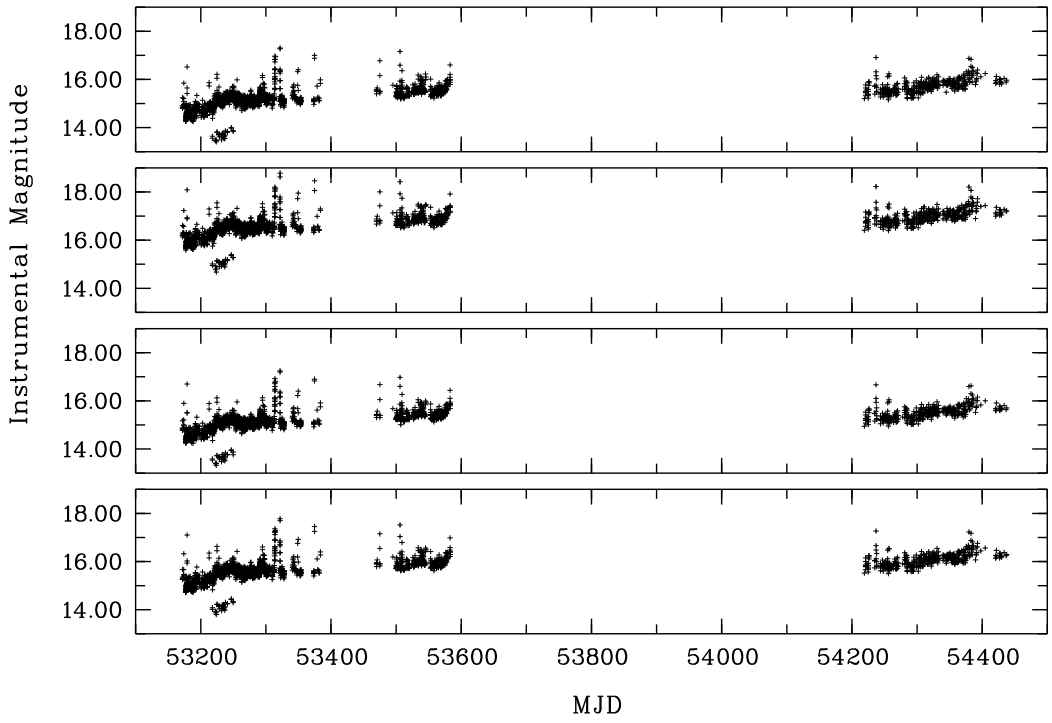

Figure 3.2: Light curves of standard stars. Lines number 1, 2 and 3 represent the first, second and third reference stars, respectively. The fourth line represents the arithmetic mean of the reference stars. The vertical bars denote the magnitude errors.

errors. The average, represented by arithmetic mean, of the refence stars is also in the figure.

The mean of the reference stars was subtracted from the light curve of the SAX J2103.5 to eliminate instrumental and weather related errors (Figure 3.3). ASM data for the same interval and 5.0-12.0 keV energy band was also given in the figure for comparison. Figure 3.4 shows an outburst from May 2007 to December 2007. The outburst's flux is given as (1.7±0.1) 10^{-9}ergcm^{-2}s^{-1} in 20-40 keV energy band by Galis et al. (2007). To obtain luminosity, using distance values of 3.2 kpc (Baykal et al. 2002) and 6.5 kpc (Reig et al. 2004) the $L = (4\pi d^2)F$ formula was applied. Thus, two luminosity values were obtained: $L_1 = 2.08 \times 10^{36}$, $L_2 = 8.59 \times 10^{36}$ ergs^{-1}. These values might indicate that the April 2007 outburst was a Type I. In Figure 3.5, the light curve of the system's optical component before and after the outburst is shown. The

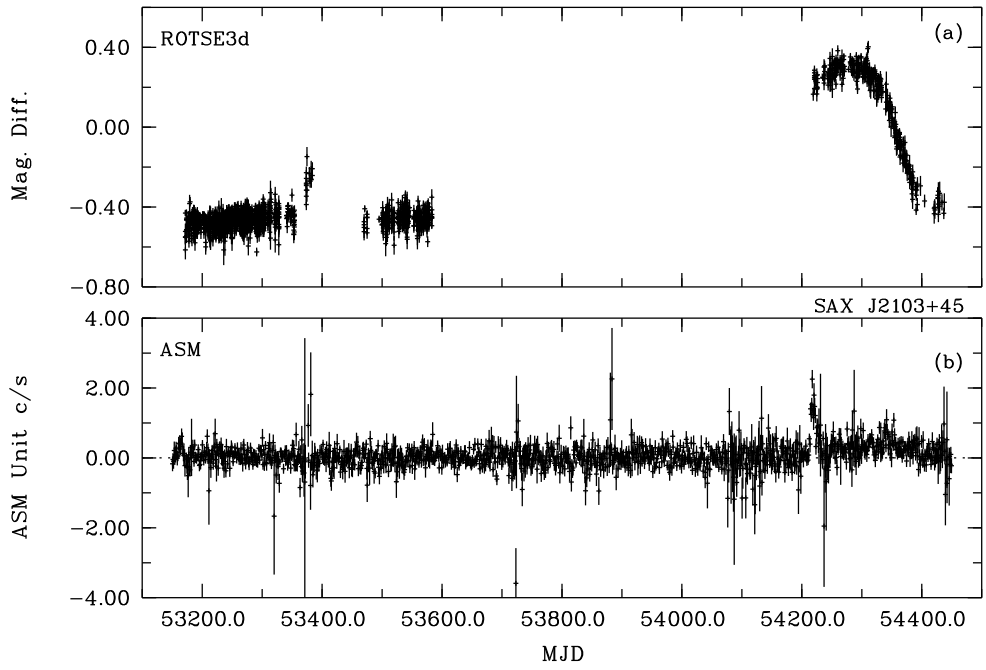

Figure 3.3: Light curve of the difference between the system's optical component and average of the reference stars (a). ASM light curve of the system in X-ray region for the same interval.

appropriate data was taken from ROTSE-IIId, and was divided into two sub-data sets, the first up to December 2007, the second from December 2007 to November 2008. The first set's magnitudes were calculated with DAOPHOT, whereas the rest of the data was extracted using SExtractor, provided by Prof. Dr. Ümit Kızıloğlu. The light curve obtained was composed of average magnitudes of seven days.

The system, which underwent an outburst in 2001, was in quiescence until May 2004, then as it can be seen in the Figure 3.3, it kept remaining in quiescence until April 2007, where an outburst happened. From the figure, it can be deducted that the X-ray and optical light curve profiles are in agreement with each other. The optical light curve indicates that there might have been another relatively small outburst in 53400 (MJD). From Figure 3.5 it can be concluded that the system went back into quiescence after the outburst in 2006.

The nine spectroscopic observations were reduced using MIDAS and its long slit and

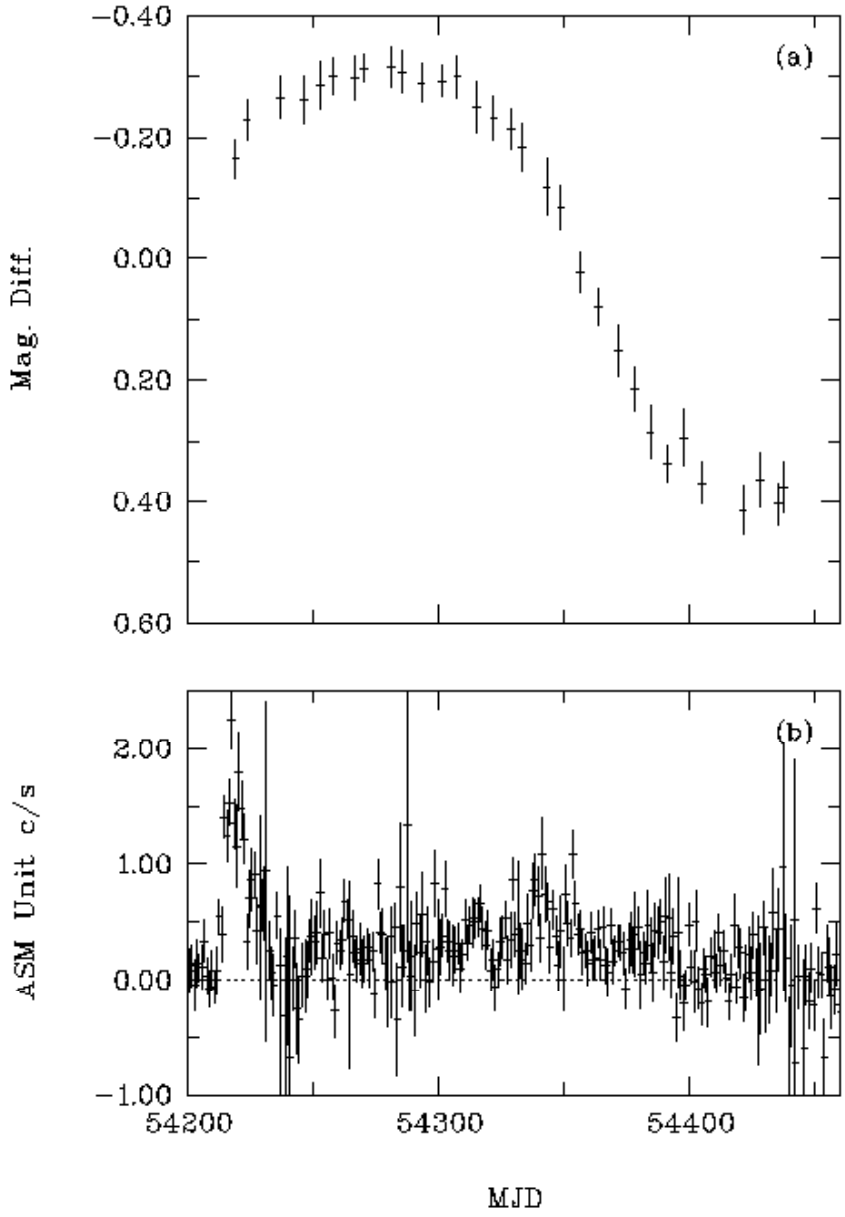

Figure 3.4: Light curve of the system's outburst using 7 day averages in 2007 along with ASM data.

ALICE packages (See Chapter 2.4.2). Three sample spectra taken using grism 8 can be seen in Figure 3.6.

Figure 3.7 shows the Hα line profiles for all eight observations made with grism 8. The y-axis denotes normalized intensity. Table 3.1 presents the properties of the lines, and also Table 3.2 shows Hα line's components' parameters. Examining the line pro-

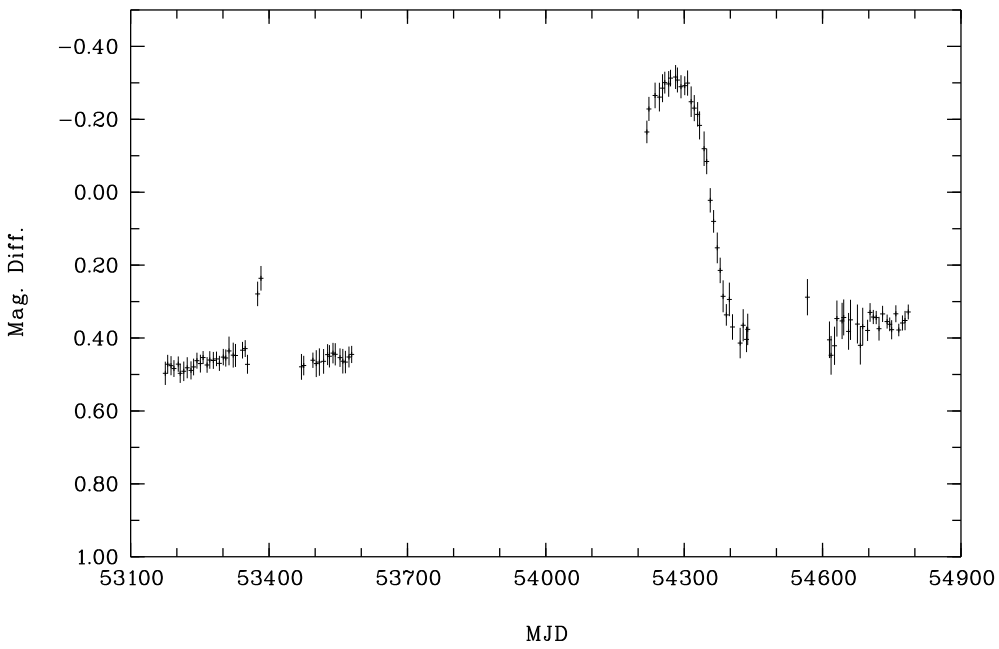

Figure 3.5: Light curve of the system pre- and post-outburst using 7 day averages.

file, the increase in strength of the emission of the Hα line can be seen up to October 2007. Then, in December 2007, the line suddenly shows an absorption profile. After that, absorption line keeps getting stronger. This change from emission to absorption points out to the existence of a circumstellar disc around the optical companion. The disc is existent as a dense structure where an emission line can be seen (June - October 2007). The density of the disc increases as the strength of the emission increases, i.e. from July 2007 to September 2007. When the line shows an absorption profile, the disc is either non-existent or exists as a rather thin structure (December 2007 - September 2008). Since SAX J2103.5+4545 is the Be/X-ray binary with the shortest period (P$\sim$12 d), its components are closer to each other compared to other Be/X-ray systems. The fastest emission-absorption reversals can be seen in SAX J2103.5+4545 due to this fact. Reig et al. (2002) stated SAX J2103.5+4545 is about 3 and 5 times faster than 4U 0115+63 and X Per, respectively.

Figure 3.8 shows the light curve of the system's optical component and the corresponding Hα equivalent widths derived from spectroscopic observations, along with

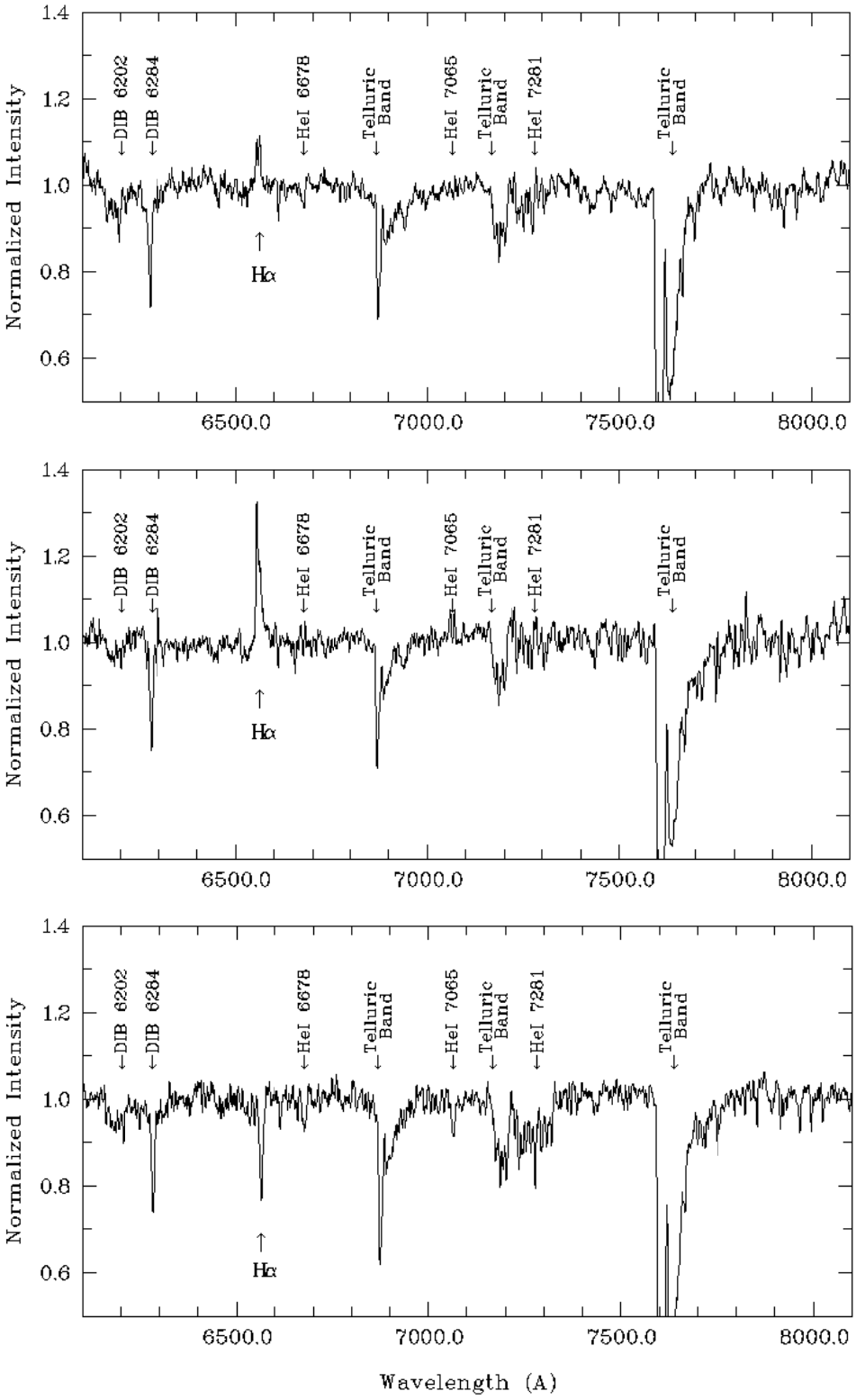

Figure 3.6: Spectra taken with G8 on 18 July 2007 (top panel), on 5 October 2007 (middle panel), on 21 September 2008 (bottom panel)

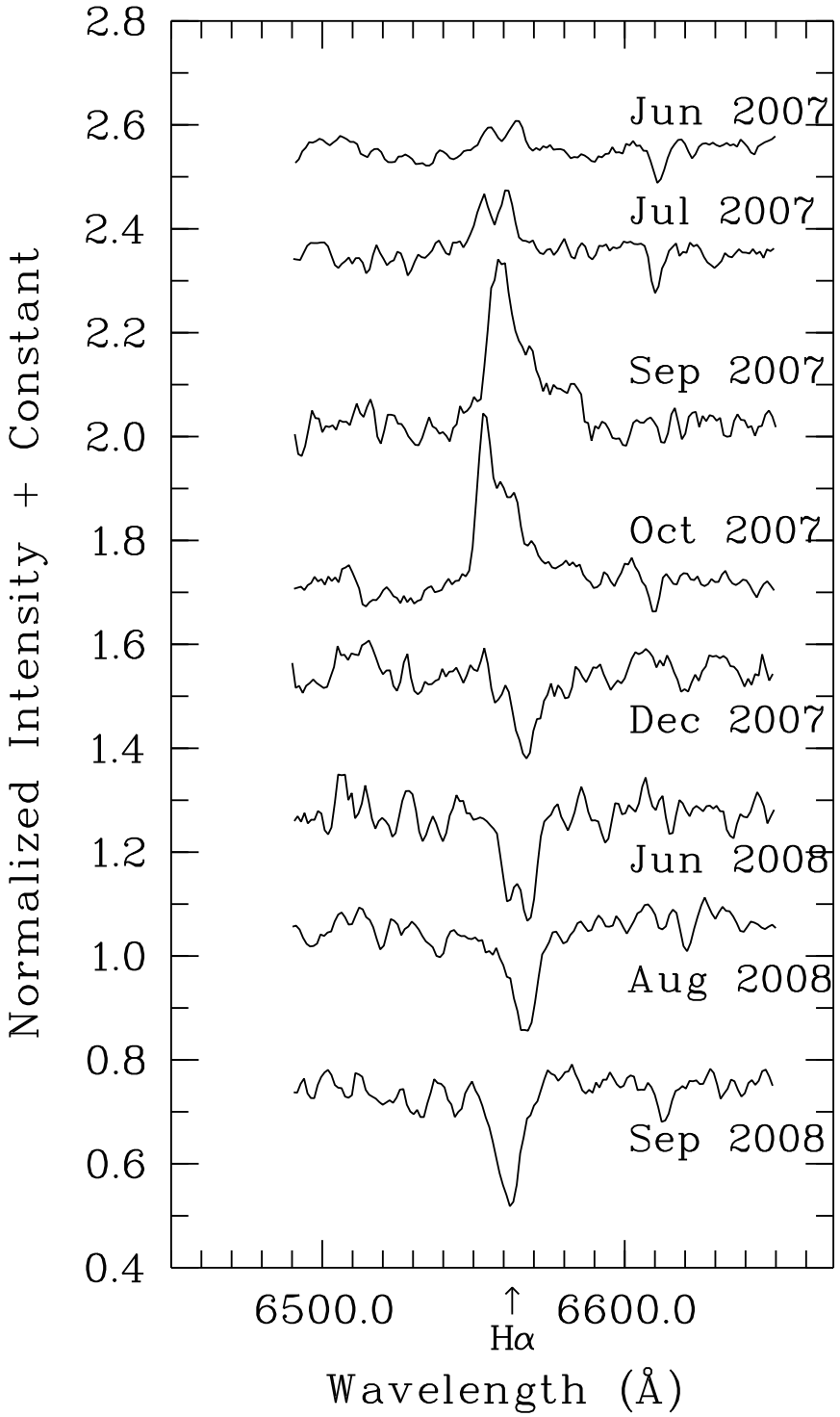

Figure 3.7: Hα profiles obtained from several spectra in 2007 and 2008.

Table 3.1: Properties of Hα line profiles.

DATE	MJD	CENTER (A°)	FWHM (A°)	EW (A°)
14 Jun. 2007	54265.9095	6560.79	14.16	0.61 ± 0.09
18 Jul. 2007	54299.8713	6657.40	15.26	1.55 ± 0.14
13 Sep. 2007	54356.8789	6561.14	18.23	5.86 ± 0.33
5 Oct. 2007	54378.7865	6557.25	15.19	4.51 ± 0.16
14 Dec. 2007	54448.8526	6567.45	10.10	-1.81 ± 0.18
19 Jun. 2008	54636.9561	6565.52	11.18	-2.17 ± 0.19
26 Aug. 2008	54705.4451	6560.10	11.54	-2.72 ± 0.17
21 Sep. 2008	54731.5074	6561.38	10.06	-2.37 ± 0.13

appropriate ASM data. Figure 3.9 displays the detailed light curve of the optical component during the outburst. Similar to Figure 3.8 Hα equivalent widths and ASM data can be seen. This figure is a modified vesion of Figure 3.4, also giving the Hα equivalent widths to check the agreement with ASM data.

The system is moderately eccentric (e=0.4), therefore, the Be star's disc extends beyond its Roche lobe during some periastron passages (Ziółlkowski 2002). The extension does not always happen because the system is not highly eccentric (e>0.6). When the extension happens, it is possible for matter to accrete on the neutron star, causing outbursts. This effect will truncate the part of the disc beyond the Roche lobe. The truncation results in highly reduced Hα emission: The equivalent width of the

Table 3.2: Properties of Hα line's components for each observation. 1 and 2 denote the first and second components of the line. 'AMP.' abrreviation is the amplitude of the line and additionally 'WID' is the width of the line in pixel units.

DATE	AMP.(1)	WID(1)	FWHM(1)	AMP.(2)	WID(2)	FWHM(2)
14 Jun. 2007	0.58	2.97	7.98	-0.57	2.66	7.14
18 Jul. 2007	0.46	3.18	8.54	-0.40	2.41	6.48
13 Sep. 2007	0.83	5.56	14.92	-0.65	4.24	11.37
5 Oct. 2007	1.38	3.64	9.77	-1.20	3.05	8.20
14 Dec. 2007	-0.14	3.76	10.10	-	-	-
19 Jun. 2008	-0.92	2.72	7.31	0.80	2.21	5.93
26 Aug. 2008	-0.19	4.30	11.54	-	-	-
21 Sep. 2008	-0.22	3.75	10.32	-	-	-

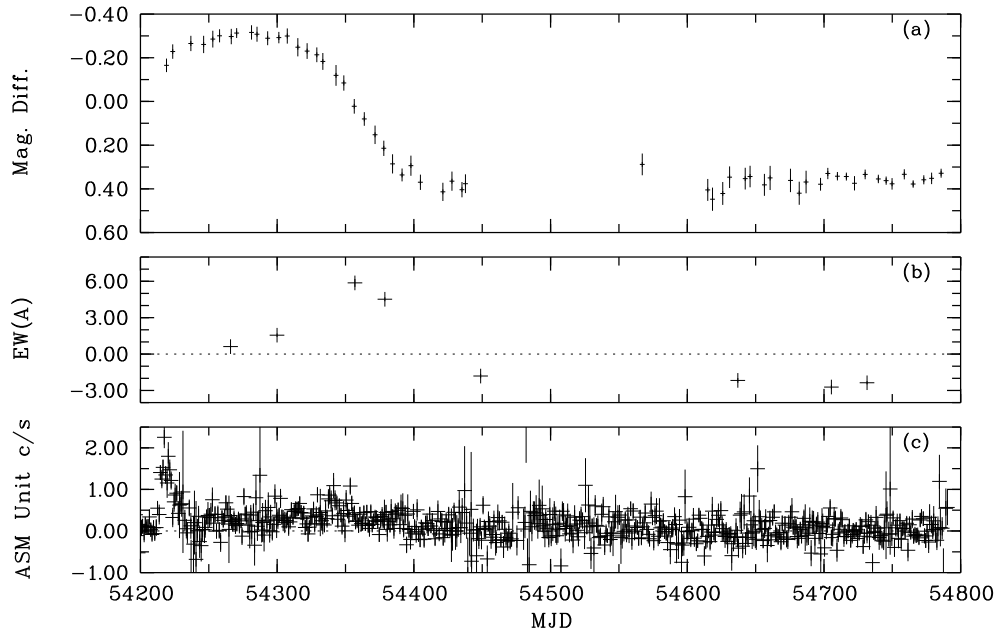

Figure 3.8: The correlation between magnitude variations of the Be star, EW of Hα line and ASM data

Hα emission during the outburst is 2.5±0.2 ang. (MJD 54234) (Manousakis, Reig and Kougentakis, 2007), whereas it is 0.61±0.09 after the outburst.

From the lower panel of Figure 3.9 it can be deduced that the outburst happened during the 54217.16 MJD periastron passage. During the outburst a large amount of matter flows from the Be star to the neutron star causing the matter to start an outburst. Afterwards, the intensity shrinks. Matter still keeps accreting around the Be star, because of this, in the middle panel of the figure, the Hα line profile shows an emission ($\sim$ 54250 MJD). After a certain point the disc becomes unstable and starts precessing. This fact combained with the moderate eccentricity and small orbital seperation results in small gaps which allow transfer of matter (Reig et al. 2004). These transfers cause the neutron star to increase activity. After some time, $\sim$100 days in our case, the disc will be exhausted of its matter and mass transfers will slow down, which will result in reduced neutron star activity. From the bottom panel of Figure 3.9, the slight increase in intensity can be seen from 54250 to 54350 MJD. Then, it slowly decreases to the regular value (54350-54400 MJD).

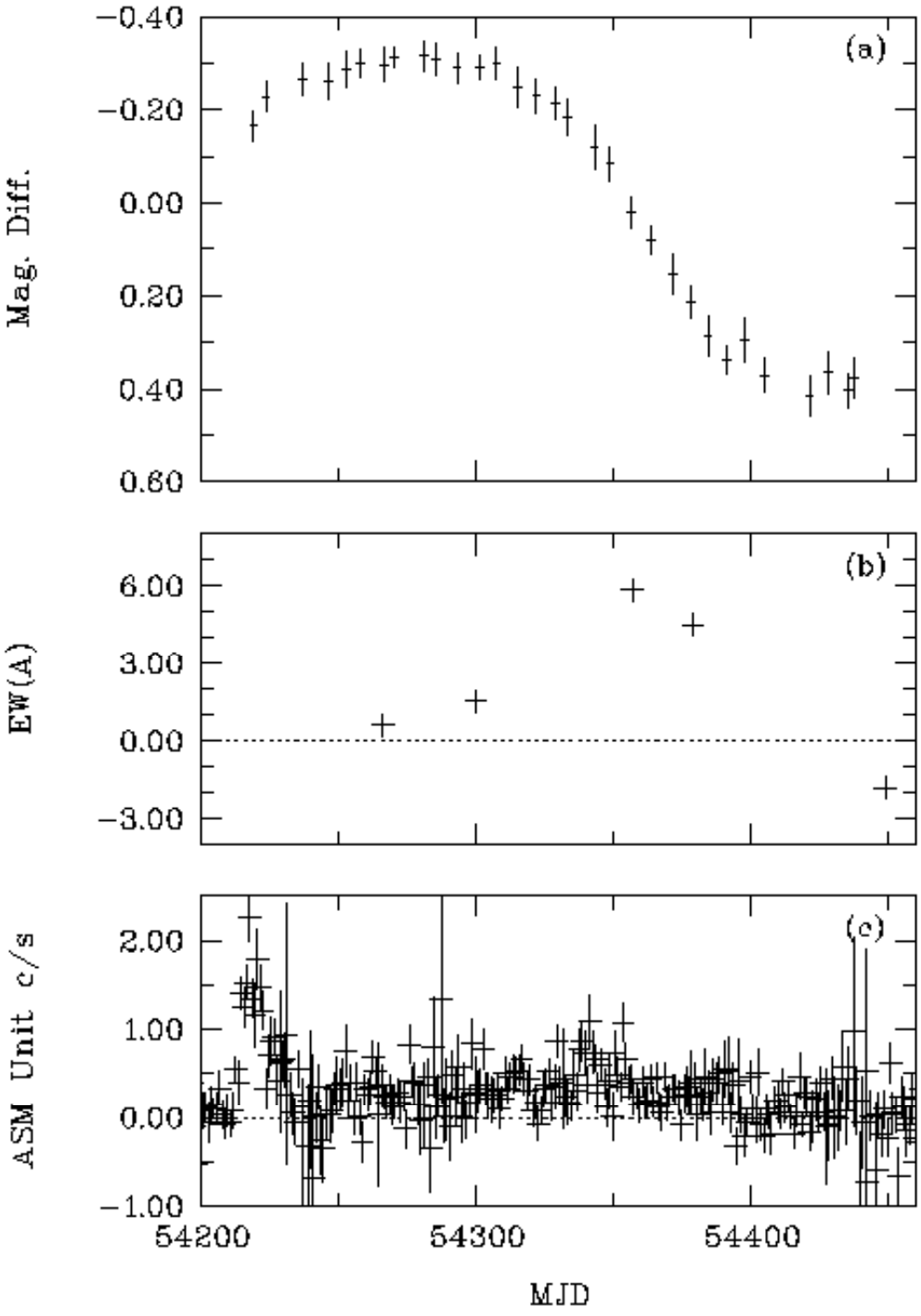

Figure 3.9: The correlation between magnitude variations of the Be star, EW of Hα line and ASM data during the outburst

CHAPTER 4

CONCLUSION

In this study the optical photometric and spectroscopic observations for SAX J2103.5+4545's optical component were presented and analyzed. The system showed several X-ray outbursts in the last ten years, some of these were Type II, e.g. 1999, 2001 whereas someothers were Type I, e.g. 2004, 2007. In this thesis, how variations of optical radiation were related to X-ray variations of the source is investigated. In April 2007 the system showed increased activity in the X-ray region, which implied an outburst. The outburst turned out to be a Type I. During the outburst optical magnitudes went up by 1^m, i.e. the system's radiation grew ~2.5 times stronger compared to the one in quiescence. And also, in this outburst, an emission in the Hα line profile was observed. This fact indicates to the presence of a decretion disc around the Be star. During the outburst the emission weakens because the Be star's disc becomes truncated by the neutron star. At the end of the outburst (October 2007) the emission in Hα increases, because the Be star keeps accreting material onto itself. Afterwards the disc becomes unstable and starts precessing and small gaps appear which leads to mass transfer. This causes the neutron star to increase X-ray activity. The mass transfer will ultimately exhaust the disc matter and the emission will wane and eventually turn into an absorption. The emission-absorption reversal happens extremely fast in SAX J2103.5+4545, because the orbital period is very short and the stars are very close to each other. The existence of the absorption implies that the Be star's disc is gone with the outburst. The system remains in quiescence since, the H-alpha line is still showing an absorption which means that there is still not enough material around the Be star to form a disc. This study reveals how SAX J2103.5+4545 effects its optical companion's properties.

REFERENCES

[1] Akerlof, C. W., Kehoe, R. L., McKay, T. A., Rykoff, E. S., Smith, D. A. et al. 2003, PASP, 115, 132.

[2] Apparao, K. M. V. 1994, SSRv, 69, 255.

[3] Baykal, A., Stark, M. J., & Swank, J. 2000, The Astrophysical Journal, 544, 129.

[4] Baykal, A., İnam, S. Ç, Stark, M. J., Heffner, C. M., Erkoca, A. E., & Swank, J. H. 2007, MNRAS, 374, 1108.

[5] Bertin, E., & Arnouts, S. 1996, Astronomy and Astrophysics Supplement Series, 117, 393.

[6] Blay, P., Reig, P., Martínez-Núñez, S., Camero, A., Connell, P., & Reglero, V. 2004, A & A, 427, 293.

[7] Blay, P., Reig, P., Martínez-Núñez, S., Camero, A., Connell, P., & Reglero, V. 2004, ESASP, 552, 273.

[8] Blay, P., Camero, A., Martínez-Núñez, S., Reig, P., & Negueruela, I. 2006, ESASP, 604, 243.

[9] Camero Arranz, A., Wilson, C. A., Finger, M. H., & Reglero, V. 2007, A & A, 473, 551.

[10] Collins, G. W. II 1987, IAU Colloquium 92, Physics of Be stars, ed. Slettebak, A. and Snow, T. P., Cambridge University Press, 3.

[11] Corbet, R. H. D. 1984, A& A, 141, 91.

[12] Corbet, R. H. D. 1986, MNRAS, 220, 1047.

[13] de Loore, C. et al. 1982, in M. Jaschek and H. -G. Groth (eds.), IAU Symp., 98, 347.

[14] Filippova, E. V., Lutoviniv, A. A., Shtykovsky, P. E., Revnivtsev, M. G., Burenin, R. A. et al. 2004, Astronomy Letters, 30, 12, 824.

[15] Finger, M. H., & Prince, T. A. 1997, Proc. Fourth Compton Symp. 1 (AIP, Woodbury, NY), 57.

[16] Galis, R., Bianchin, V., Grebenev, S., McBreen, B., Mereghetti, S., et al. 2007, ATel # 1063, 1G.

[17] Habets, G. M. H. J. 1986, A& A, 165, 95.

[18] Hulleman, F., in't Zand, J. M. M., & Heise, J. 1998, A& A, 337, 25.

[19] İnam, S. Ç, Baykal, A., Swank, J., & Stark, M. J. 2004, The Astrophysical Journal, 616, 463.

[20] Kızıloğlu, Ü., Kızıloğlu, N., & Baykal, A. 2005, The Astrophysical Journal, 130, 2766.

[21] Lee, U., Saio, H., & Osaki Y. 1991, MNRAS, 250, 432.

[22] Levine, A. M., Bradt, H., Cui, W. et al. 1996, The Astrophysical Journal, 496, L33.

[23] Li, X. -D., & van den Heuvel, E. P. J. 1996, A& A, 314L, 13.

[24] Lutovinov, A., Molkow, S, & Revnivtsev, M. 2003, arXiv:astro-ph/0306289.

[25] Manousakis, A., Reig, P., & Koungentakis, A. 2007, ATel # 1063, 1M

[26] Negueruela, I., & Okazaki, A. T. 2000, ASP Conference Series, 214, 713.

[27] Negueruela, I. 2004, arXiv:astro-ph/0411335.

[28] Okazaki, A. T., & Negueruela, I. 2001, ASP Conference Series, 234, 281.

[29] Okazaki, A. T., & Negueruela, I. 2001, A& A, 377, 161.

[30] Okazaki, A. T., & Hayasaki, K. 2006, ESASP, 604, 171.

[31] Porter, J. M. 1998, A& A, 336, 966.

[32] Pringle, J. E. 1996, MNRAS, 281, 357.

[33] Rappaport, S., & van den Heuvel, E. P. J. 1982, in M. Jaschek and H. -G. Groth (eds.), 'Be stars', IAU Symp., 98, 327.

[34] Reig, P., & Roche, P. 1999, MNRAS, 306,100.

[35] Reig, P. 2004, ESASP, 552, 373.

[36] Reig, P., Negueruela, I., Fabregat, J., Chato, R., Blay, P., & Mavromayakis, F. 2004, A& A, 421, 673.

[37] Sidoli, L., Mereghetti, S., Larsson, S., Chernyakova, M., Kreykenbohm, I. et al. 2004, ESASP, 552, 475.

[38] Sidoli, L., Mereghetti, S., Larsson, S., Chernyakova, M., Kreykenbohm, I. et al. 2005, A & A, 440, 1033.

[39] Slettebak, A. 1988, PASP, 100, 770.

[40] Stella, L., White, N. E., & Rosner, R. 1986, The Astrophysical Journal, 308, 669.

[41] Stetson, P. B. 1987, PASP, 99, 191.

[42] Stetson, P. B. 1992, ASCPC, 25, 297.

[43] Waters, L. B. -F. M., & Van Kerkwijk, M. H. 1989, A& A, 223, 196.

[44] Ziółkowski, J. 2002, MmSAI, 73, 1038z.